Simple cubic three-dimensional photonic crystals based on macroporous silicon and anisotropic posttreatment

Sven Matthias,[a] Frank Müller, and Ulrich Gösele
Max Planck Institute of Microstructure Physics,[b] *Weinberg 2, Halle 06120, Germany*

(Received 3 May 2005; accepted 9 June 2005; published online 1 August 2005)

Three-dimensional structures for photonic crystal applications have been fabricated up to now either by pure bottom-up approaches such as colloidal self-assembly, by pure top-down approaches using very large scale integration technology, or by interference lithography. Here we evaluate a concept enabling large photonic band gaps in simple cubic structures, the manufacturing of which is based on photoelectrochemical etching of strongly modulated macroporous silicon. A subsequent anisotropic etching of the porous structure, which exploits the crystallographic nature of the substrate used, converts the former circular cross section of the pores into a squared one. We theoretically study the dispersion behavior of photonic crystals being fabricated by this developed technique. The band-structure calculations are compiled with respect to the relative pore arrangement and the dielectric volume fraction. We present experimentally realized structures and characterize the photonic crystal optically. The reflectance measurements are in good agreement with corresponding band-structure calculations. Moreover, the introduced process extends the variety of designing and sculpturing three-dimensional microstructures to meet the requirements of a multitude of micro- and nanotechnological applications.
[DOI: 10.1063/1.1993752]

I. INTRODUCTION

Manufacturing of periodic three-dimensional structures with micrometer dimensions and nanometer precision has gained more and more importance in the rapidly growing field of photonic band-gap materials[1,2] but also found some applications in other areas, e.g., for Brownian ratchets.[3] Recently, three-dimensional photonic crystals—periodic structures with a varying dielectric constant in three dimensions—were intensively investigated due to the modification of the spontaneous emission[4,5] and the promise to possibly revolutionize telecommunication as a result of their unusual optical properties.[6,7] Different kinds of three-dimensional photonic crystals have been proposed and were fabricated, e.g., the woodpile structure with diamond symmetry, realized by layer-by-layer methods[8] or the inverted opal structures of fcc symmetry, fabricated by sintering of submicron spheres and backfilling the voids with a high-index material.[9,10]

Simple cubic photonic crystals are attractive due to their easy integration in top-down approaches and the realization via very large scale integration (VLSI) technology.[11] In particular, the well-established self-stabilized photoelectrochemical etching of deep macropores in silicon is a very promising technique to shape silicon quickly and reliably.[12,13] The arrangement of the pores is determined flexibly by the lithographically defined arbitrary two-dimensional lattice on the silicon surface. Moreover, the macropore etching in *n*-type silicon wafers allows changing the diameter of the pores during the growth resulting in three-dimensional structures.[3,14] Pores with strong diameter variations could be fabricated by an advanced photoelectrochemical etching, in which the shape of each period is determined by the applied etching current and voltage profiles[15] as shown in Fig. 1. A subsequent isotropic postprocessing converted this columnar structure into a simple cubic network of intersecting air spheres in silicon. The corresponding theoretical and optical characterizations[16] indicated a complete band gap of 4%. The advantages of three-dimensional macroporous silicon-based photonic crystals for the infrared spectral range are the precise and fast fabrication—20 lattice constants in depth and millions lateral take only 1 h.

With respect to optical applications a larger band gap than the reported 4% would be desirable. Here we evaluate a concept enabling larger photonic band gaps in simple cubic structures, manufacturing of which is nevertheless based on macroporous silicon. An anisotropic posttreatment of the initial macroporous silicon sample will exploit the crystallo-

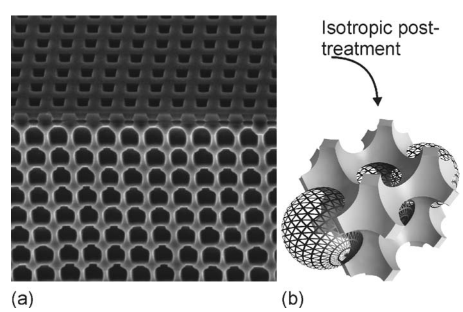

FIG. 1. (a) Scanning electron microscopy (SEM) picture of strongly modulated pores in macroporous silicon arranged in a cubic primitive lattice with a lattice constant of 2 μm. Initial structure before a further postprocessing. (b) Model of a simple cubic lattice of air spheres in silicon obtained by an isotropic erosion (based in Ref. 16).

[a]Author to whom correspondence should be addressed; electronic mail: matthias@mpi-halle.mpg.de
[b]url: http://www.mpi-halle.de

graphic nature of the silicon single crystal used in the photoelectrochemical etching process. The former circular cross section could hence be converted by this method into a squared one. Such a quadratic pore shape establishes the large area fabrication of two kinds of simple cubic photonic crystals. Before finally presenting the experimentally realized structures, a detailed theoretical investigation will be given, focusing on photonic band structures.

II. ANISOTROPIC ETCHING

Photoelectrochemical etching and isotropic posttreatment have proven to be versatile techniques to fabricate three-dimensional structures in silicon.[16] For example, this approach allows to fabricate a columnar structure of air pores arranged in a simple cubic lattice in (001)-oriented *n*-type silicon wafers. The diameter of these cylindrical pores is strongly modulated and varies between 0.8 and 1.75 μm with a period that equals the lateral lithographically defined lattice constant [Fig. 1(a)]. Isotropic erosion, by several oxidization and subsequent etching steps, transfers this columnar structure into the simple cubic lattice of overlapping air spheres.

Besides the illumination profile during the etching and the isotropic erosion, there exists a further degree of freedom to shape silicon. The crystallography of the silicon single crystal used enables an anisotropic post treatment of these three-dimensionally shaped macroporous silicon samples with an alkaline solution. Potassium hydroxide (KOH)—the alkaline solution used here—etches in the $\langle 100 \rangle$ and $\langle 110 \rangle$ directions, two orders of magnitude faster than in the $\langle 111 \rangle$ direction[17] resulting in cubic structures with squared cross section. Such a cross section of the pores breaks the cylindrical symmetry and hence the relative orientation with respect to the axes of the square lattice arrangement of the pores becomes important. Either the sidewalls of the pores are close to each other [Fig. 2(a)] or the corners of them [Fig. 2(c)]. If the sidewalls are parallel to the axes of the square lattice, the anisotropic widening should lead to a scaffoldlike structure of dielectric bars with squared cross section along all Cartesian axes, which penetrate each other in one point [Fig. 2(b)]. Compared to the original scaffold structure[18] there exists a rotation of the bars by 45° along their longitudinal axes.

III. SIMULATIONS

We calculated the corresponding band structure [Fig. 3(a)] with the MIT package.[19] The result indicates a complete photonic band gap between the 2nd and the 3rd bands of 5% gap to midgap ratio (assuming a refractive index of silicon with $n_{\mathrm{Si}}=3.4$). The maximum gap size is reached at a filling ratio of air of 84% or equally at a width of the bars $s=0.27a$, where a is the lattice constant. This band gap is stable and present for bars with a width from $s=0.21a$ up to $s=0.38a$ [Fig. 3(b)]. This scaffoldlike structure resembles the well-known scaffold structure introduced in 1993 by Sözüer and Haus[18] and realized in 2002 by Lin *et al.*[1] However, in our case there is the rotation of bars around their longitudinal axes, which affects obviously the geometry but hardly the optical properties. The band gap is very stable with respect to a varying width of the bars. A change of ±22% is acceptable until the band gap is closed.

As described above, the pore arrangement can also be

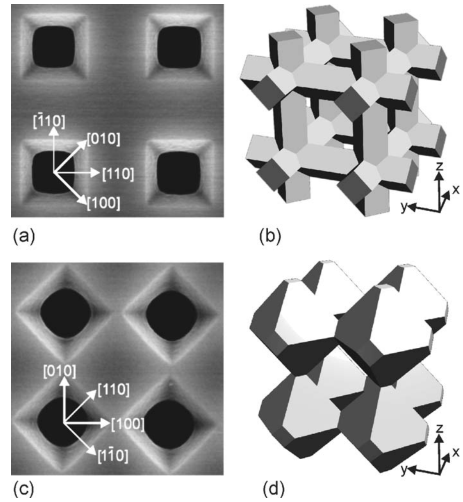

FIG. 2. SEM pictures of lithographically prestructured silicon surfaces and model structures. (a) Square lattice of pores in silicon with a pitch of 2 μm. The sides of the KOH pits are parallel to the axes of the square lattice. (b) Three-dimensional (3D) model of a dielectric scaffoldlike structure consisting of bars with squared cross section rotated around their longitudinal axes. (c) Square lattice of pores in silicon with a lattice constant $a=1.5$ μm. The KOH pits are rotated by an angle of 45° against the axes of the square lattice so that the corners are close to each other. (d) 3D model of intersecting air octaeders.

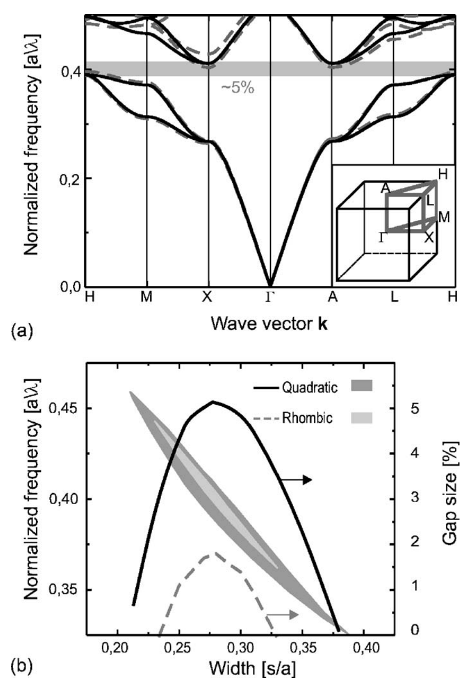

FIG. 3. Band-structure and band-gap map calculations of the scaffoldlike structure. (a) Band structure of a scaffoldlike structure consisting of bars with squared cross section (solid) and bars with rhombic cross sections in the *x*-*y* plane and squared cross section in *z* direction (dashed). The inset shows the irreducible Brillouin zone for a tetragonal lattice. The parameter *s* is equivalent to the width of the dielectric bars. (b) Band-gap map of the scaffoldlike structures with squared bars (dark area and solid) or for rhombic bars in the *x*-*y* plane and squared bars in *z* direction (light gray area and dashed).

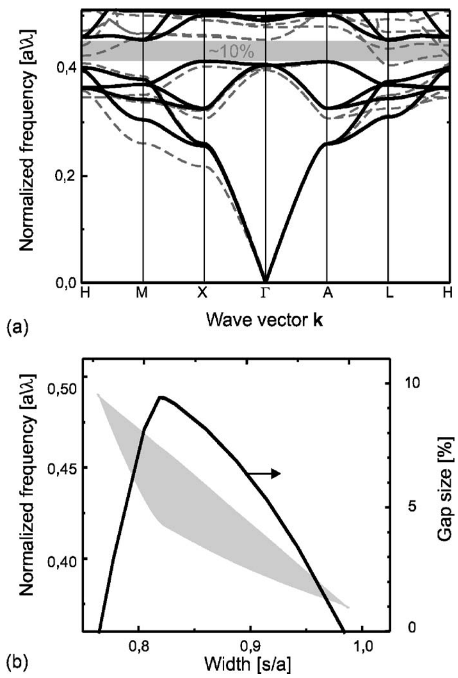

FIG. 4. Band-structure and band-gap map calculations of the overlapping air octaeder structure. (a) Band structure for the simple cubic case (solid) and the tetragonal case (dashed). The parameter s reflects the width of the intersecting air octaeder (b) Band-gap map for the simple cubic case.

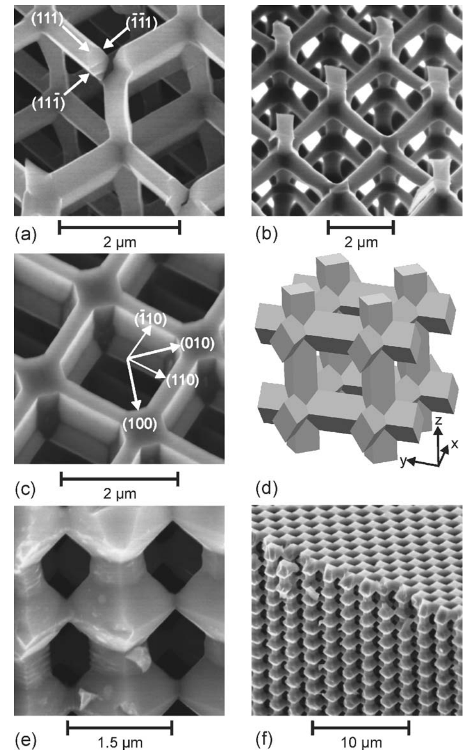

FIG. 5. SEM pictures of cubic three-dimensional photonic crystals in macroporous silicon. (a) Side view of the scaffoldlike structure. The surfaces of the bars in the x and y directions are formed by the $\{111\}$ planes of the silicon crystal. (b) Bird's eye view of the scaffoldlike structure obtained by anisotropic widening of macroporous silicon. (c) Top view. The bars along the z direction have $\{100\}$-oriented surfaces. (d) Model of this scaffoldlike structure with tetragonal symmetry. (e) and (f) Resulting overlapping air-octaeder structure.

rotated by 45° relative to the axes of the square lattice as shown in Fig. 2(c). Under these conditions anisotropic etching leads to quite strong scatterers that are connected at the edges. These structures are similar to the arrangements that have been investigated theoretically by Biswas *et al.*[20] They demonstrated that networks consisting of cubically arranged dielectric bodies with interconnecting thin dielectric bars possess band gaps with a gap to midgap ratio of 12% between the 5th and the 6th bands. The recently proposed simple cubic *P* structure[21]—with smooth and round edges—belongs also to this category. For our own calculations we approximate the etched structure by intersecting air octaeders as schematically shown in Fig. 2(d). The corresponding band-structure calculation [Fig. 4(a)] indicates a broad frequency range, where light propagation is forbidden. The complete gap accomplishes a relative width of 10% between the 5th and the 6th bands [Fig. 4(b)].

IV. EXPERIMENT

The experimental posttreatment of the porous sample is carried out in an alkaline solution. To prevent inhomogeneities along the pore due to concentration gradients a membrane structure of macroporous silicon was prepared.[22] This enables the alkaline solution ($c_{\mathrm{KOH}}=2$ wt%) to flow through the tiny channels and precludes any concentration gradient, which would evolve if the bulk silicon closes the bottom of the pores. Limiting the mass transfer to diffusion would finally cause inhomogeneities. Figures 5(a)–5(c) show the resulting scaffoldlike structure. The alkaline solution creates flat crystallographic surfaces starting from the porous silicon matrix. The network resembles the model presented in Fig. 2(b). However, the resulting scaffoldlike structure differs in some aspects from the theoretically proposed one. The assumed bars with squared cross section were obtained along the growth direction (z direction) of the pores. The surfaces of these bars are the $\{100\}$ planes of the silicon single crystal. In the x-y plane of the macroporous silicon, along the x and the y directions of the photonic crystal, the cross section of the bars is rhombic [Fig. 5(a)]. The surfaces are formed by the $\{111\}$ planes of the single crystalline substrate, which are not orthogonal to each other but include an angle of about 109°. The different surfaces of the bars along the x and y directions on the one hand and the z direction on the other hand cause different etching rates. Thus, a well-adjusted initial macroporous silicon sample is required to meet the assumption that finally all the bars have the same width.

The crystallographic nature of the substrate used influences the second type, proposed above, of simple cubic structure along the z direction in a similar manner [Figs. 5(e) and 5(f)]. Instead of the octaeder-shaped air volume an elongated double pyramid is obtained, because the surfaces are formed by the $\{111\}$ planes of the silicon crystal.

V. DISCUSSION

Adding anisotropic pore widening to the fabrication process enables a degree of freedom for the design of photonic crystals. This may be used to produce quite a variety of structures as presented in Fig. 5. In particular, by combining the introduced technique with isotropic etching and the

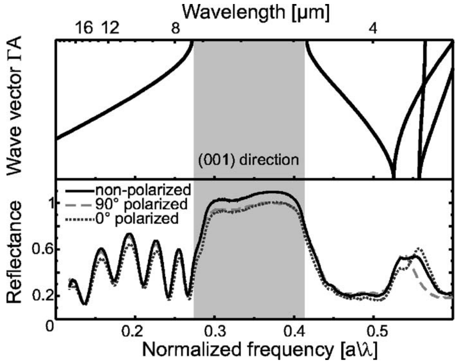

FIG. 6. Optical characterization of the resulting scaffold structure in Figs. 5(a)–5(c). The region of the fundamental band gap for this direction of propagation is highlighted in gray.

widely adjustable initial pore shape we may obtain many more geometries in the future. Although the anisotropic etching behavior enables the fabrication of squared cross sections along the z direction, the symmetry of the final structure is not simple cubic, due to the nonorthogonality of the $\{111\}$ planes. The rhombic cross section of the bars in the x-y plane reduces the symmetry of our structure to a tetragonal one. This affects the optical properties. For the calculation of the band structure we assumed a modified geometrical model, which consists of the rhombic bars in the x-y plane and bars with squared cross section in z direction. All bars have the same width and the lattice constant is equal for all directions. This special geometry still has a complete band gap, but it is reduced to a 2% gap to midgap ratio for a filling fraction of 84% air [Fig. 3(a)]. Furthermore the size range of the bars, in which a complete gap appears, shrinks [Fig. 3(b)].

As mentioned above, the rhombic cross section of the bars in the x-y plane reduces the symmetry and thus the gap size. Considering these bars as stretched squares along the z direction motivates a compensation of the stretching by reducing the lattice constant in this direction. However, the calculations showed that, although there is a small effect, the complete band gap is not increased significantly and is still around 2%. Finally, a band gap is present for a lattice constant l_z in z direction in a range from $l_z=0.95a$ to $l_z=1.02a$.

Optical characterization of this structure was performed along the z direction with a Fourier transform infrared (FTIR) microscope (Bruker Optics) (Fig. 6). The Fabry-Perot oscillations indicate the high quality of our photonic crystal structure. The range of enhanced reflectance coincides very well with the calculated band structure for this direction suggesting an achievable complete band gap of 2%. No polarization dependence was observed as expected for the propagation along the z direction, because the symmetry is fourfold. The influence of the crystallography on the overlapping air-octaeder structure is fairly dramatic, because the band gap between the 5th and the 6th gaps is quite sensitive to the symmetry. Our calculation, which is based on the modified geometry taking into account the crystallographic-determined elongation of the octaeder, demonstrates that there is no complete band gap present anymore [Fig. 4(b)]. However, there is a broad frequency band over a large range of k points, where the light propagation is forbidden. This may be of interest for directed emission in random lasing applications.

VI. CONCLUSION

We presented theoretical and experimental investigations of three-dimensional photonic crystals possessing simple cubic and tetragonal symmetries with squared cross sections. It was demonstrated that simple cubic symmetry theoretically enables large band gaps up to 10%. An approach was made to fabricate these structures using strongly modulated macroporous silicon and anisotropic widening in an alkaline solution. The crystallography of the substrate used allows the growth of structures with tetragonal symmetry resulting in smaller band gaps. However, the introduced concept of the anisotropic posttreatment opens the possibility to fabricate a variety of shapes besides the known air spheres. Combining the presented anisotropic posttreatment with the isotropic one and keeping the arbitrarily adjustable initial pore shape of the macroporous silicon in mind establishes a versatile sculpturing technique of complex three-dimensional structures in silicon that may be used in future photonic crystal applications.

ACKNOWLEDGMENTS

The authors thank Professor R. B. Wehrspohn, Dr. V. Lehmann, Professor S. John, and Dr. T. Chan for their support and for discussions. The authors are grateful to Ms. Sklarek for her assistance in the laboratory. This project was partly financed by a research award for young scientists given by the state of Saxony-Anhalt.

[1] E. Yablonovitch, Phys. Rev. Lett. **58**, 2059 (1987).
[2] S. John, Phys. Rev. Lett. **58**, 2486 (1987).
[3] S. Matthias and F. Müller, Nature (London) **424**, 53 (2003).
[4] P. Lodahl, A. F. van Driel, I. S. Nikolaev, A. Irman, K. Overgaag, D. van Maekelbergh, and W. L. Vos, Nature (London) **430**, 654 (2004).
[5] S. Ogawa, M. Imada, S. Yoshimoto, M. Okano, and S. Noda, Science **305**, 227 (2004).
[6] H. Kosaka, T. Kawashima, A. Tomita, M. Notomi, T. Tamamura, T. Sato, and S. Kawakami, Phys. Rev. B **58**, R10096 (1998).
[7] M. Soljacic and J. D. Joannopoulos, Nat. Mater. **3**, 211 (2004).
[8] K. M. Ho, C. T. Chan, C. M. Soukoulis, R. Biswas, and M. Sigalas, Solid State Commun. **89**, 413 (1994).
[9] H. S. Sözüer, J. W. Haus, and R. Inguva, Phys. Rev. B **45**, 13962 (1992).
[10] J. E. G. J. Wijnhoven and W. L. Vos, Science **281**, 802 (1998).
[11] S. Y. Lin, J. G. Fleming, R. Lin, M. M. Sigalas, R. Biswas, and K. M. Ho, J. Opt. Soc. Am. B **18**, 32 (2001).
[12] V. Lehmann, J. Electrochem. Soc. **140**, 2836 (1993).
[13] V. Lehmann and H. Föll, J. Electrochem. Soc. **137**, 653 (1990).
[14] V. Lehmann and U. Grüning, Thin Solid Films **297**, 13 (1997).
[15] S. Matthias, F. Müller, J. Schilling, and U. Gösele, Appl. Phys. A: Mater. Sci. Process. **80**, 1391 (2005).
[16] S. Matthias, F. Müller, C. Jamois, R. B. Wehrspohn, and U. Gösele, Adv. Mater. (Weinheim, Ger.) **16**, 2166 (2004).
[17] V. Lehmann, *Electrochemistry of Silicon* (Wiley, Weinheim, 2002).
[18] H. S. Sözüer and J. W. Haus, J. Opt. Soc. Am. B **10**, 296 (1993).
[19] S. G. Johnson and J. D. Joannopoulos, Opt. Express **8**, 173 (2001).
[20] R. Biswas, M. M. Sigalas, K. M. Ho, and S. Y. Lin, Phys. Rev. B **65**, 205121 (2002).
[21] C. K. Ullal, M. Maldovan, E. L. Thomas, G. Chen, Y. J. Han, and S. Yang, Appl. Phys. Lett. **84**, 5434 (2004).
[22] S. Matthias, J. Schilling, K. Nielsch, F. Müller, R. B. Wehrspohn, and U. Gösele, Adv. Mater. (Weinheim, Ger.) **14**, 1618 (2002).